Δελτίο της Ελληνικής Γεωλογικής Εταιρίας, τομ. XLVII , 2013
Πρακτικά 13ου Διεθνούς Συνεδρίου, Χανιά, Σεπτ. 2013

Bulletin of the Geological Society of Greece, vol. XLVII 2013
Proceedings of the 13th International Congress, Chania, Sept. 2013

SYNTHESIS AND CHARACTERIZATION OF FOUR NEW HALLOYSITE–TIO_2 NANOCOMPOSITES

Papoulis D.[1], Komarneni S.[2], Toli D.[1], Panagiotaras D.[3] and Bakalis S.[1]

[1] *University of Patras, Department Geology, Papoulis@upatras.gr*

[2] *The Pennsylvania State University, Department of Ecosystem Science and Management and Materials Research Institute, Materials Research Laboratory, University Park, PA 16802, USA*

[3] *Technological Educational Institute of Patras, Department of Mechanical Engineering, 26334, Patras, Greece*

Abstract

The synthesis as well as the characterization of small-sized TiO_2 particles supported on Halloysite are presented. Hallloysite from Utah, USA as well as from Limnos, island Greece, were used to synthesize two nanocomposites for each halloysite with TiO_2 to halloysite weight ratios of 80: 20 and 60:40 and compare with published data of well formed nanocomposites of intermediate proportion (70-30) that were previously studied. All nanocomposites were prepared by deposition of anatase (TiO2) on the halloysite tubes using a sol–gel method under hydrothermal treatment at 180 °C. Phase composition, particle morphology and physical properties of these samples were characterized using X-Ray Diffraction (XRD), Scanning Electron Microscopy (SEM), Attenuated Total Reflection using Fourier Transform Infrared spectroscopy (ATR-FTIR) and N_2 surface area analysis by BET. Preparation of all halloysite–TiO2 nanocomposites led to the anticipated good dispersion of anatase particles on halloysite surfaces. ATR-FTIR results revealed the formation of hydrogen bonding between anatase and the outer surfaces of halloysite tubes. All halloysite-TiO2 nanocomposites largely showed interparticle mesopores of about 5.7nm and high SSAs.

Key words: *Anatase, clay minerals, Photocatalytic activity.*

Περίληψη

Η σύνθεση και ο χαρακτηρισμός των νανοσύνθετων TiO_2 αποτεθειμένων σε αλλοϋσίτη παρουσιάζονται σε αυτήν την εργασία. Χρησιμοποιήθηκε αλλοϋσίτης από τη Γιούτα (Η.Π.Α.) και από τη νήσο Λήμνο για τη σύνθεση δύο νανοσύνθετων για κάθε αλλοϋσίτη με αναλογίες μάζας TiO_2 προς αλλοϋσίτη 80:20 και 60:40 και να συγκριθούν με δεδομένα από καλοσχηματισμένα νανοσύνθετα με ενδιάμεσες αναλογίες (70:30) που έχουν παρασκευαστεί, χαρακτηριστεί και δημοσιευθεί στο παρελθόν. Όλα τα νανοσύνθετα παρασκευάστηκαν με απόθεση ανατάση στους επιμήκεις κρυστάλλους αλλοϋσίτη χρησιμοποιώντας μία μέθοδο διαλύματος-πυκτώματος σε υδροθερμική επεξεργασία στους 180 °C. Η ορυκτολογική ανάλυση, η μορφολογία των κρυστάλλων και οι φυσικές ιδιότητες προσδιορίστηκαν με τη χρήση περιθλασιμετρίας ακτίνων Χ, ηλεκτρονικού μικροσκοπίου σάρωσης, υπέρυθρης φασματοσκοπίας μετασχηματισμού κατά Fourier και προσδιορισμός της ειδικής επιφάνειας με τη μέθοδο BET. Η προετοιμασία όλων των νανοσύνθετων οδήγησε στη

επιθυμητή καλή διασπορά των κρυστάλλων ανατάση πάνω στις επιφάνειες των κρυστάλλων του αλλοϋσίτη. Από την υπέρυθρη φασματοσκοπία μετασχηματισμού κατά Fourier προσδιορίστηκε ο σχηματισμός δεσμών υδρογόνου μεταξύ του ανατάση και των εξωτερικών επιφανειών του αλλοϋσίτη. Μετά την επεξεργασία όλα τα νανοσύνθετα εμφάνισαν κυρίων μεσοπόρους μεγέθους περίπου 5.7nm και υψηλή ειδική επιφάνεια.
Λέξεις κλειδιά: *Ανατάσης, αργιλικά ορυκτά, φωτοκατάλυση.*

1. Introduction

It is well known that TiO_2 nanoparticles have good catalytic activities because of their large specific surface areas where reactions take place (Zhao et al., 2006). Titanium dioxide, especially in the form of anatase, has proven to be the most suitable semiconductor for widespread environmental applications such as the degradation of oil spills and the decomposition of many organic molecules as well as other air pollutants (Hoffmann et al., 1995; Michael et al., 1995; Fujishima et al., 2000; Martínez-Ortiz et al., 2003). TiO_2 powders, however, easily agglomerate into larger particles, reducing their photocatalytic activities (Zhao et al., 2006).

Clay minerals are attractive materials for adsorption and catalysis (Chmielarz et al., 2011) and when composited with TiO_2, they have been used in aqueous dispersions to enhance the removal of organic pollutants by photocatalytic degradation (Mogyorósi et al., 2002; Kibanova et al., 2009), as well as to increase the photocatalytic activities in decomposing air pollutants (e.g. Nikolopoulou et al., 2009; Papoulis et al., 2010; Papoulis et al., 2013a; Papoulis et al., 2013b). Previous investigations revealed that using clay minerals with microfibrous (Aranda et al., 2008; Karamanis et al., 2011) or tubular morphology (Papoulis et al., 2010; Papoulis et al., 2013a; Papoulis et al., 2013b) as a template and TiO_2 as the photocatalyst led to significantly increased TiO_2 photocatalytic activity in decomposing many pollutants. The dispersion of anatase nanoparticles onto halloysite surfaces under mild conditions is a promising method to resolve the agglomeration problem of TiO_2 (Papoulis et al., 2010; Papoulis et al., 2012). Recent studies showed that halloysite-TiO_2 nanoparticles have excellent photocatalytic activities in decomposing both inorganic and organic air pollutants (Papoulis et al., 2010; Papoulis et al., 2013b).

In present work, we describe the synthesis and characterization of nano-sized TiO_2 particles supported on two different halloysites (weight ratios of TiO_2 to Halloysite were 80:20 and 60:40) by using a novel method under mild conditions, which does not involve calcinations or stabilizing agents. The results are compared with recently published data for well prepared nanocomposites of different TiO_2-Halloysite proportions (70-30) that show very high photocatalytic activities in decomposing air and organic pollutants (Papoulis et al., 2013b). The aim of this study was to prepare well formed clay-based nanocomposites that could have increased photocatalytic efficiency in decomposing inorganic and organic air pollutants.

2. Materials and Methods

2.1. Sample Preparation

A halloysite sample from Utah, USA and a halloysite sample from Limnos island were used in this study. Both the samples were size fractionated to obtain <2 μm by gravity sedimentation followed by centrifugation to separate solid from liquid.

2.2. TiO_2 Stock Sol Dispersion

A stock TiO_2 sol dispersion was prepared by mixing titanium tetraisopropoxide, $Ti(OC_3H_7)_4$, with hydrochloric acid, nanopure water (3D) and absolute ethanol (Langlet et al., 2003). The TiO_2 stock dispersion was diluted in absolute ethanol to give a 0.05 M concentration of $Ti(OC_3H_7)_4$.

2.3. Halloysite-supported TiO_2

An aliquot of TiO_2 sol was stirred for 2 h and then the (1% w/w) halloysite-water dispersion was added to the TiO_2 dispersion in order to obtain the desirable TiO_2 content. The slurry was stirred for 24 h and the resulting dispersion was centrifuged for 10 min (3800 rpm) followed by three times centrifuge washing (with 3D water). The halloysite–TiO_2 composites were then dispersed in a 1:1 water:ethanol solution, prior to hydrothermal treatment in an autoclave for 5 h at 180 °C. The products were centrifuged for 15 min (at 3800 rpm) and oven-dried for 3 h (at 60 °C).

2.4. Characterization

The phase compositions of untreated and TiO_2 treated halloysite samples were determined by X-ray diffraction (using a Bruker D8 advance diffractometer, with Ni-filtered CuKα radiation). XRD patterns were obtained from oriented or random powder samples in a 2θ range of 2° to 60° at a scanning rate of 2 °/min. Random powder mounts for selected samples were prepared by gently pressing the powder into the cavity holder. Oriented clay powder samples were prepared by the dropper method. Halloysite-TiO_2 morphology was examined with a SEM LEO SUPRA 35VP. Attenuated total reflection infrared (ATR/FTIR) measurements were made with the ATR Miracle accessory of PIKE technologies (diamond crystal) attached to the EQUINOX 55 FT-IR spectrometer (BRUKER). Nitrogen adsorption-desorption isotherms for each sample degassed at 100 ^{o}C for 3 hours were obtained at 77K using Autosorb^{-1} (Quantachrome corporation). Brunauner-Emmet-Teller (BET) surface areas and pore size distribution were determined from the isotherms. Pore size distribution of each sample was obtained using density functional theory (DFT) method in which a N_2 adsorption branch model was selected.

3. Results and Discussion

3.1. X-Ray Diffraction

Both halloysite samples (from Utah and Limnos island), as it has been reported in previous studies, are pure with no detectable impurities, if any (not detected by XRD) (Papoulis et al., 2013b). Figure 1 shows the XRD patterns of the four nanocomposites prepared in this study from both halloysites compared with nanocomposites 70-30. All patterns show the presence of dehydrated halloysite and anatase, confirming their phase purity (Figure 1). The XRD patterns of all nanocomposites showed all the characteristic reflections of anatase (γ-TiO_2) at 25.3°, 37.9°, 47.6°, 54.8° 2θ, which intensity decreasing by decreasing TiO_2 amount. Additionally the intensity of the 001 reflection of dehydrated halloysite is increasing with increasing amount of dehydrated halloysite. The XRD patterns also indicated that the temperature of 180 °C involved in the synthesis of halloysite-TiO_2 nanocomposites did not modify the native mineral structure of dehydrated halloysite. It is well known that heating halloysite at 100-350 ^{o}C sharpens the basal reflection (001) and reduces the spacing but never to as low as the characteristic reflection of kaolinite (7.14 Å) (Brindley and Robinson, 1946; Joussein et al., 2005). In this study, the basal reflections of both halloysites after treatment were detected at 7.29 Å (Figure 1).

3.2. ATR-FTIR Spectra

The ATR-FTIR spectra of all four TiO_2-treated halloysites compared with nanocomposites 70-30 from both areas are generally similar (Figure 2), while the intensities of halloysite reflections are lower in the nanocomposites and especially in the nanocomposites with the lower amounts of halloysite (20%) in them. The reflections of the spectra confirm that the structures of both dehydrated halloysites were not changed after treating with TiO_2. None of the characteristic bands of dehydrated halloysite (Joussein et al., 2005; Bobos et al., 2001) were affected except the Si–O broad stretching band which shifted from about 997 cm^{-1} (Papoulis et al., 2010) to more than 1000 cm^{-1} (Figure 2) in all nanocomposites. The shifting of the Si–O broad stretching band increased with increasing amount of anatase (Figure 2). This shift is an indication of the formation of

hydrogen bonding between TiO_2 and the outer surfaces of halloysite tubes (tetrahedral sheet) which becomes stronger in the more anatase rich nanocomposites. The ATR-FTIR spectra of all nanocomposites confirmed that the treatment temperature of 180°C during the synthesis of halloysite-TiO_2 nanocomposites did neither destroy halloysites nor modified their native dehydrated halloysite mineral structure.

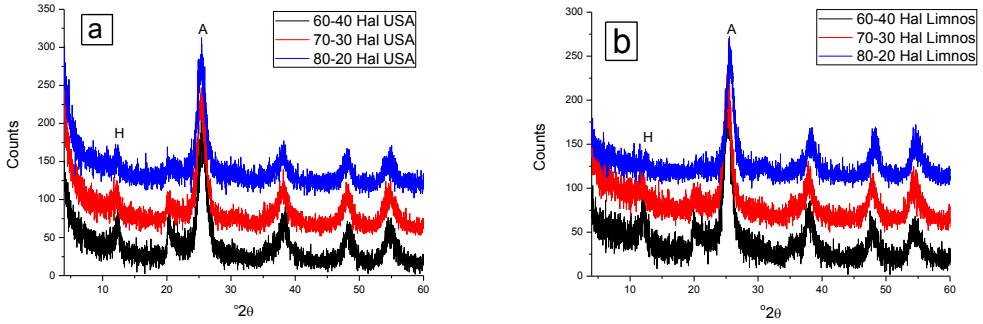

Figure 1 – XRD patterns of the four new Halloysite-TiO_2 nanocomposites (60-40, 80-20) from both areas compared with the two previously studied nanocomposites (70-30) a) nanocomposites using halloysite from Utah and b) nanocomposites using halloysite from Limnos (H: halloysite, A: anatase).

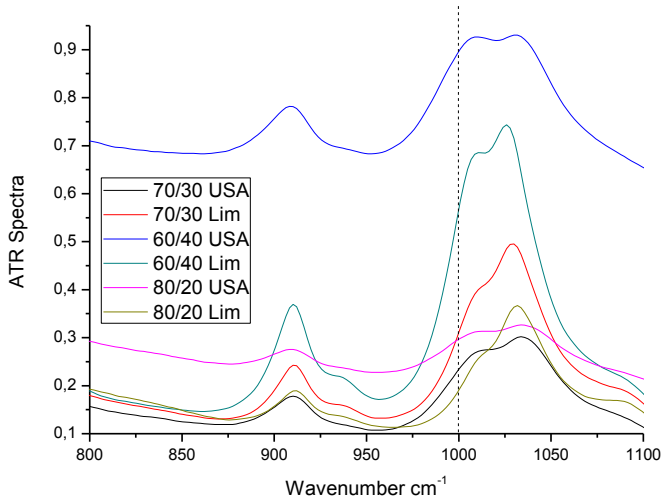

Figure 2 – ATR-FTIR Spectra of Halloysite-TiO_2 nanocomposites compared with the two previously studied nanocomposites (70-30) (Lim:Limnos).

3.3. Scanning Electron Microscopy (SEM) and Transmission Electron Microscopy (TEM)

In this investigation we present SEM micrographs of the four nanocomposites compared with nanocomposites 70-30 (Figure 3), while the morphologies of both halloysites have already been previously reported by us (Papoulis et al., 2010; Papoulis et al., 2013b). It should be noted that the halloysite tubes from Limnos island appear to be well formed (Papoulis et al., 2010), while those from Utah are not curved and rolled up that perfectly. The latter morphology, therefore, suggests

that more halloysite surfaces are available for TiO_2 nanoparticles to be dispersed in the sample from Utah (Papoulis et al., 2013b).

SEM observations of all nanocomposites showed that many uniform TiO_2 grains of about 10-30 nm were deposited on the external surfaces of halloysite tubes of all nanocomposites (Figure 3). The TiO_2 nanoparticles were found to be distributed very well on both halloysite external surfaces but not homogeneously (Figure 3) although homogeneous distribution of TiO_2 grains on halloysite tubes was anticipated (Papoulis et al., 2013b). TiO_2 nanoparticles seem to cover, at least partially, the lumen of most halloysite tubes (Figure 3). By increasing the amount of TiO_2 content, the deposited TiO_2 particles were found to be aggregated on the surfaces of the halloysite tubes (Figure 3) while decreasing the amount of TiO_2 led to aggregation of halloysite tubes from both sources.

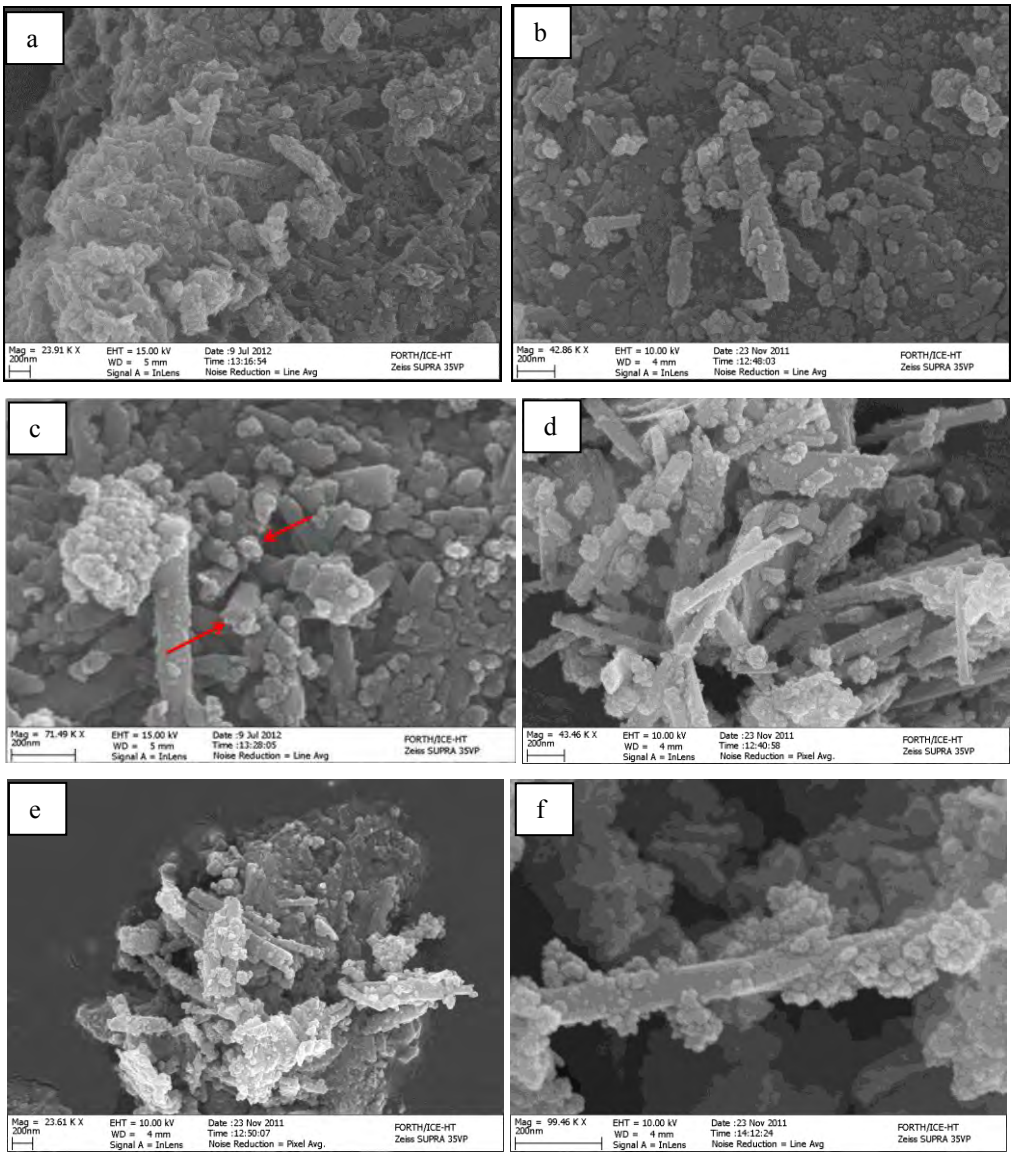

Figure 3 – SEM micrographs of Halloysite-TiO_2 nanocomposites from Utah (a: 60-40, b: 70-30, c: 80-20) and Limnos island (d: 60-40, e: 70-30, f: 80-20) (arrows: anatase nanoparticles partially covering halloysite lumen).

3.4. Determination of Specific Surface Areas (SSAs) and Porosity

Adsorption–desorption isotherms of nitrogen and pore size distributions for all four halloysites–TiO_2 nanocomposites compared with nanocomposites 70-30 are presented in Figures 4 and 5 and Figures 6 and 7, respectively. The isotherm shapes for all nanocomposites are of the same type (type IV) indicating both meso and micropores (IUPAC classification, 1994) (Sing et al., 1985; Sing et al., 2004). The different size of the hysteresis observed is due to the different proportions of halloysite and anatase, two minerals with major differences in size, shape and SSA. Additionally the two different halloysites are characterized by differences in size and SSA. The total pore volumes of the nanocomposites with halloysite from Utah were found to be significantly higher while the SSAs were found to be slightly smaller than those of the nanocomposites with halloysite from Limnos (Figures 6, 7). This could be attributed to the presence of more interparticle pores (macroporous) of the first samples while the second type of samples show more mesopopores at about 5.7 nm (Figures 6, 7) and retained the higher SSA (of halloysite from Utah) due to a better TiO_2 distribution on halloysite external surfaces. All nanocomposites largely showed mesopores of about 5.7 nm, while the macropores found in starting halloysite material (Papoulis et al., 2010) were considerably reduced apparently due to partial covering of the lumen of halloysite tubes by TiO_2 nanoparticles.

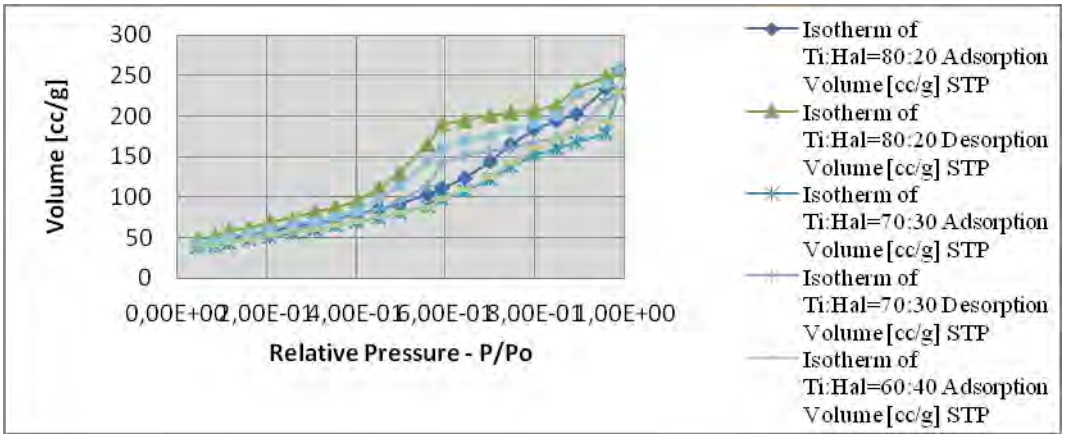

Figure 4 - Adsorption-desorption isotherms of nitrogen for nanocomposites using halloysite from Utah compared with the two previously studied nanocomposite (70-30).

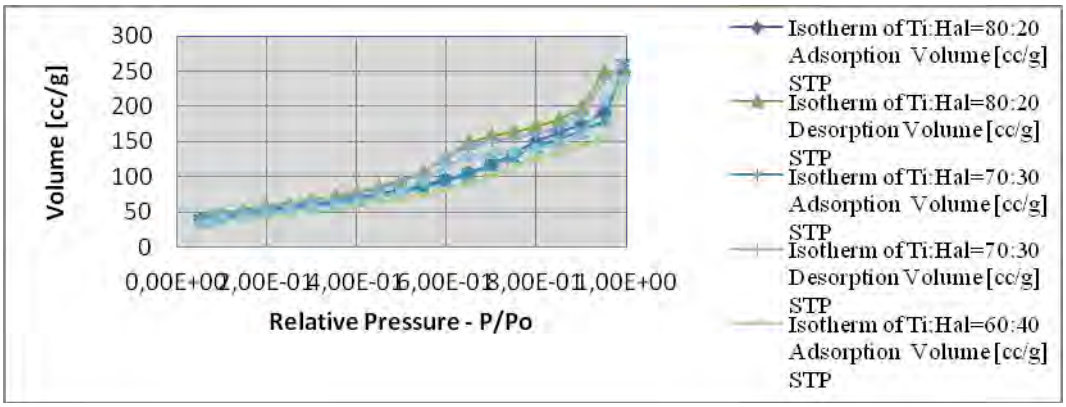

Figure 5 - Adsorption-desorption isotherms of nitrogen for nanocomposites using halloysite from Limnos compared with the previously studied nanocomposite (70-30).

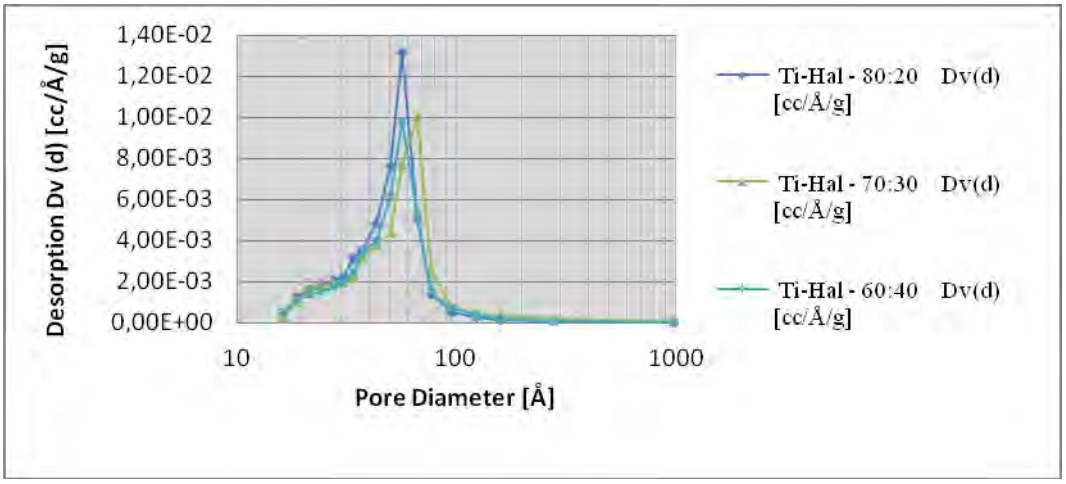

Figure 6 - Pore size distribution for nanocomposites using halloysite from Utah compared with the previously studied nanocomposite (70-30).

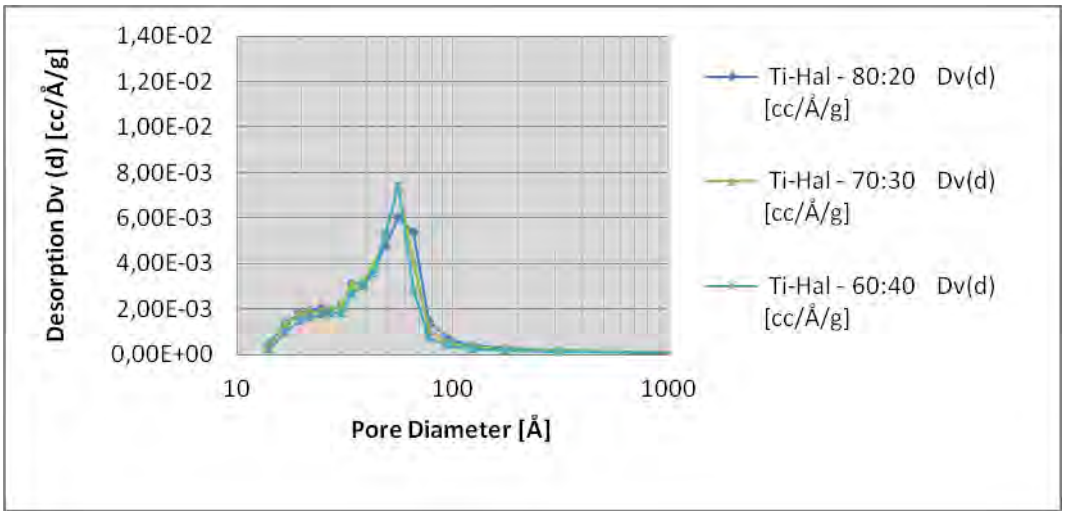

Figure 7 - Pore size distribution for nanocomposites using halloysite from Limnos compared with the previously studied nanocomposite (70-30).

4. Conclusions

Preparation of four new halloysite–TiO_2 nanocomposites using two different halloysites led to good dispersion of anatase on the external surfaces of halloysite tubes. Both halloysites were not destroyed by the treatment temperature, while the formation of hydrogen bonding between the outer surfaces of halloysite tubes and TiO_2 was detected. All nanocomposites largely showed interparticle mesopores of about 5.7nm. The characteristics of the nanocomposites presented here compared with the characteristics of already tested samples in different TiO_2-Halloysite proportion (70-30) that were presented in our recently published paper (Papoulis et al., 2013b) suggest promising photocatalytic activities in decomposing organic as well as inorganic air pollutants.

5. Acknowledgments

The authors would like to acknowledge financial support from the European Union (Lead Market European Research Area Network - LEAD ERA) and the Regional Authority of Western Greece

under the project ″Development and manufacturing of a new innovative nanotechnology-based decontaminant construction material for indoor building - INDOOR ECOPAVING″. The project is implemented under the Operational Programme "DEPIN 2007-2013" Priority Axis (PA) 'Digital convergence and entrepreneurship in Western Greece', action "Transnational Business Collaboration Western Greece" and is co-funded by the European Union –European Regional Development Fund and National Resources (NSRF 2007-2013).

The authors would like to thank Dr. Drakopoulos of the Foundation for Research and Technology-Hellas (FORTH) Institute of Chemical Engineering and High Temperature Chemical Processes (ICE/HT) Rio-Patras, Greece, for his help with SEM micrographs.

6. References

Aranda P., Kun R., Martín-Luengo M. A., Letaïef S., Dékány I., and Ruiz-Hitzky E. 2008. Tiatania-sepiolite nanocomposites prepared by a surfactant templating colloidal route, *Chem. Mater*., 20, 84-91.

Brindley G.W. and Robinson K., 1946. Randomness in the structures of kaolinitic clay minerals, *Tran. of the Far. Soc.,* 42B, 198-205.

Bobos I., Duplay J., Rocha J. and Gomes C. 2001. Kaolinite to halloysite-7 Å transformation in the kaolin deposit of Sao Vicente de Pereira. Portugal, *Clays and Clay Miner*., 49, 596-607.

Chmielarz L., Piwowarska Z., Kustrowski P., Węgrzyn A., Gil B., Kowalczyk A., Dudek B., Dziembaj R. and Michalik M. 2011. Comparison study of titania pillared interlayered clays and porous clay heterostructures modified with copper and iron as catalysts of the DeNOx process, *Appl. Clay Sci*., 53, 164-173.

Fujishima A., Tata N.R.and Donald A.T. 2000. Titanium dioxide photocatalysis, *J. Photochem. Photobio. C*., 1, 1–21.

Hoffmann M.R., Martin S.T., Choi W. and Bahnemann D.W. 1995. Environmental application of semiconductor photocatalysis, *Chem. Rev*., 95, 69–96.

Joussein E., Petit S. Churchman J., Theng B., Righi D.and Delvaux B. 2005. Halloysite clay minerals – A review, *Clay Miner.,* 40, 383-426.

Rouquerol J., Avnir D., Fairbridge C.W., Everett D.H., Haynes J.H., Pernicone N., Ramsay J.D.F.,
Sing K.S.W. and Unger K.K. 1994. Recommendations for the characterization of porous solids, IUPAC Recommendations, Technical Report, *Pure and Appl. Chem.,* 66, 1739-1758

Karamanis D., Ökte A.N., Vardoulakis E.and Vaimakis T. 2011. Water vapor adsorption and photocatalytic pollutant degradation with TiO_2-Sepiolite nanocomposites, *Appl. Clay Sci.,* 53, 181-187.

Kibanova D., Trejo M., Destaillats H. and Cervini-Silva J. 2009. Synthesis of hectorite–TiO_2 and kaolinite–TiO_2 nanocomposites with photocatalytic activity for the degradation of model air pollutants, *Appl. Clay Sci*., 42, 563-568.

Langlet M., Jenouvrier P., Kim A., Manso M. and Trejo-Valdez M. 2003. Functionality of aerosol-gel deposited TiO_2 thin films processed at low temperature, *J. Sol–Gel Sci. Technol*., 26, 759–763.

Martínez-Ortiz M.J., Fetter G. and Domínguez J.M. 2003. Catalytic hydrotreating of heavy vacuum gas oil on Al- and Ti-pillared clays prepared by conventional and microwave irradiation methods, *Mesopor. Mater*., 58, 73–80.

Michael R.H., Scot T.M., Wonyong C. and Detlef W.B. 1995. Environmental applications of semiconductor photocatalysis, *Chem. Rev*., 95, 69–96.

Mogyorósi K., Farkas A., Dékány I., Ilisz I. and Dombi A. 2002. TiO2 based photocatalytic degradation of 2-chlorophenol adsorbed on hydrophobic clay, *Environ. Sci. Technol*. 36, 3618–3624.

Nikolopoulou A., Papoulis D., Komarneni S., Tsolis-Katagas P., Panagiotaras D., Kacandes G.H., Zhang P., Yin S. and Sato T. 2009. Solvothermal Preparation of TiO_2/Saponite Nanocomposites and Photocatalytic Activity, *Appl. Clay Sci,*. 46, 363-368.

Papoulis D., Komarneni S., Panagiotaras D.and Katsuki H. 2012. Halloysite-TiO_2 nanocomposites: Synthesis and Characterization, *Modern Management of Mine Producing, Geology and Environmental Protection*, SGEM, Bulgary, 3, 459-466.

Papoulis D., Komarneni S., Panagiotaras D., Nikolopoulou A., Christoforidis K.C., Fernández-Garcia, HuiHui Li, Yin S. and Sato T. 2013a. Palygorskite-TiO_2 nanocomposites: Part 2. Photocatalytic Activities in decomposing air and organic pollutants, *Appl. Clay Sci.* (in press).

Papoulis D., Komarneni S., Panagiotaras D., Stathatos E., Toli D., Christoforidis K.C., Fernández-Garcia, HuiHui Li, Yin S., Sato T. and Katsuki H. 2013b. Halloysite-TiO_2 nanocomposites: Synthesis, characterization and photocatalytic Activity, *Appl. Catal. B. Env.,* 132-133, 416-422.

Papoulis D., Komarneni S., Nikolopoulou A., Tsolis-Katagas P., Panagiotaras D., Kacandes G.H., Zhang P., Yin S., Sato T. and Katsuki H. 2010. Palygorskite- and Halloysite-TiO_2 nanocomposites: Synthesis and Photocatalytic Activity, *Appl. Clay Sci.,* 50, 118-124.

Sing K.S.W., Everett D.H., Haul R.A.W., Moscou L., Pierotti R.A., Rouquerol N. and Siemieniewska T. 1985. Reporting physisorption data for gas/solid systems with special reference to the determination of surface area and porosity, *Pure Appl. Chem*., 57, 603–619.

Sing K.S.W. and Williams R.T. 2004. The use of molecular probes for the characterization of nanoporous adsorbents, *Part. Part. Syst. Charact*., 71–79.

Zhao D., Zhou J. and Liu N. 2006. Characterization of the structure and catalytic activity of copper modified palygorskite/TiO_2 (Cu_2+-PG/TiO_2) catalysts, *Mater. Sci. Eng*., A 431, 256–262.